Available online at www.sciencedirect.com

ScienceDirect

Procedia CIRP 13 (2014) 320 – 326

www.elsevier.com/locate/procedia

2nd CIRP Conference on Surface Integrity (CSI)

Residual Stresses in Milled β-Annealed Ti6Al4V

T. Grove[a]*, J. Köhler[a], B. Denkena[a]

[a]Leibniz Universität Hannover, Institute of Production Engineering and Machine Tools, An der Universität 2, 30823 Garbsen, Germany
* Corresponding author. Tel.: +49 511 762 3930; fax: +49 511 752 5115. *E-mail address*: grove@ifw.uni-hannover.de

Abstract

Residual stresses can cause part distortion especially in the case of large components such as structural parts in aerospace industry. Therefore, this paper investigates the machining induced residual stresses for milling of a workpiece material with increasing usage in industry, the β-annealed titanium alloy Ti6Al4V. This thermal treatment results in a large grained material structure. For this reason X-ray diffraction, the standard residual stress measurement method, cannot be used for stress determination. In this paper an adopted indirect measurement method, the layer removal method is discussed. With respect to the material removal, two different methods are investigated, electrochemical material removal and laser ablation. Finally, the influence of the tool wear on the residual stress state after face milling is analyzed.

Keywords: Residual stress; milling; titanium; indirect measurement method

1. Introduction

Titanium alloys offer favorable properties for various applications and are widely used for high performance applications, especially in aerospace industry. Besides carbon fiber reinforced plastics and aluminum, the classical airplane construction material, titanium alloys are the most widely used materials in aircrafts of the newest generation. However, their properties, in particular low thermal conductivity and low elastic modulus, high chemical reactivity and serrated chip formation result in low machinability [1]. For the case of large airplane structural parts the part distortion due to residual stresses is challenging [2, 3].

Titanium material for aircraft applications is often heat-treated above the β-transus temperature (T_β = 1003°C for Ti6Al4V) to enhance fracture toughness and reduce crack propagation. In this domain, large grains with cubic body-centered elementary cells form. Cooling down below T_β, the material forms lamellae of β in a matrix of hexagonal closest packed α-titanium. The structure of the former β-grains is still visible in cross sections and is still often denominated as grain size although it is not a grain size in its original sense [4, 5]. This article follows this convention. Figure 1 presents scanning electron micrographs of a polished cross section of the investigated material. The alloy is Ti6Al4V and the material was heat-treated 30°C above T_β for t > 30 min. Afterwards a stress reliving annealing was carried out. As it can be seen the average grain size amounts to K_g = 800 µm. Large former β-grains exhibit a fine structure of plate-like β-titanium in a matrix of secondary α-titanium.

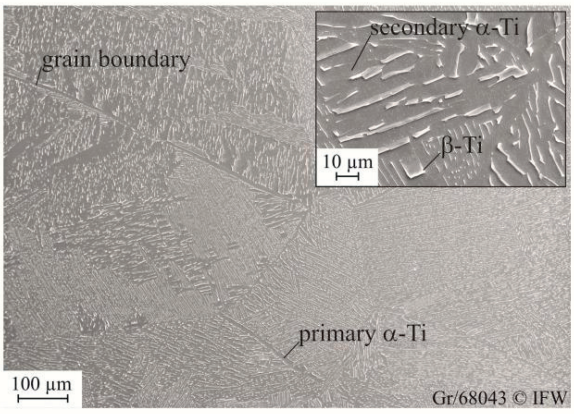

Fig 1. SEM-micrograph of a cross section of Ti6Al4V (β-annealed)

doi:10.1016/j.procir.2014.04.054

2. Residual stress measurement in large grain titanium

Measurement methods utilizing the lattice parameter to determine residual stresses are called direct measurement methods. Diffraction of radiation (X-ray, neutron diffraction, et cetera) is measured for different incidence angles ψ and subsequently the residual stress can be calculated via lattice parameter comparison with unstressed material. In contrast, indirect measurement methods are based on the determination of resulting changes in the material due to the extraction of material. For example, the layer removal methods utilizes the strain due to removal of stress inherent material [6, 7, 8].

The next chapter discusses possibilities and characteristics of different measurement methods for the case of large grained titanium material. Furthermore, a suitable solution is presented.

2.1. Direct measurement methods

Table 1 lists the different available direct measurement methods. X-ray diffractometry after the $\sin^2\psi$-method is the standard measurement technology for the residual stress determination. Some preconditions have to be fulfilled for this method. Due to statistical analysis of the deflected X-ray beam a reasonable number of material grains has to be in the measurement focus. Most diffractometers have a spot size diameter of $d \approx 2$ mm. In case of heat-treated titanium as described in the introduction less than 10 grains are focused. Furthermore, the grains have to be oriented randomly and no texture should be given enabling a constantly high number of material grains in reflection position for each value of ψ. Therefore, the standard $\sin^2\psi$-method on X-ray diffractometers cannot be applied for large grained material.

The X-ray wavelength is determined by the radiation source utilized depending on the material investigated. In contrast to this, the wavelength in a synchrotron can be continuously adjusted. Due to the much higher source power, the spot size can be enlarged up to several millimeters still remaining reasonable power density. However, due to the rare availability of such devices and the resulting high measurement costs, synchrotron radiation cannot be used standardly.

Besides X-ray also the deflection of electron and neutron beams can be utilized for the residual stress characterization. The penetration depth of these particular beams depends on the particle energy and amounts to 600-1,000 nm for electron radiation and to $t > 10$ mm for the case of neutron diffraction. Both values are not suitable to characterize process induced residual stresses which typically evolve in $t < 0.5$ mm. Electron diffraction can be carried out in scanning electron microscopes equipped with EBSD-technology (electron backscatter diffractometry). However, typical spot size of such devices is $d = 1\text{-}2$ µm to ascertain sufficient SEM-resolution. Therefore, only residual stresses in between single material grains (second kind residual stresses) can be determined.

Table 1. Direct methods for residual stress measurement

method	radiation	information depth t
X-ray diffraction	X-ray	~5 µm
synchrotron X-ray diffraction	X-ray	~5 µm
electron diffraction	electrons	~ 0.6-1.0 µm
neutron diffraction	neutrons	> 10 mm

As the available diffractometer has an X-radiation diameter of $d = 2$ mm, the resulting measuring spot forms elliptic with a conjugate diameter of $d_{con} = 2$ mm and a transverse diameter of $d_{tr} \geq 2$ mm, in dependence of the entrance angle ψ. However, the number of grains in the measured area is still < 10 for the case of the investigated material with a grain size of $d_{gr} \approx 0.8$ mm. Different techniques are evaluated to enlarge the number of material grains measured. Linear oscillation of the specimen in one and two directions is used as well as the application of so-called Komakhov-lenses for the widening of the X-ray radiation. Drawback of both methods is the reduced intensity due to widening of radiation with constant power resulting in higher measuring times. A preliminary test for two different focus sizes was carried out to investigate if the $\sin^2\psi$-method is suitable to measure residual stresses in the large grain titanium alloy investigated. Therefore, two specimens were flank milled under standard conditions and residual stresses were measured firstly with the conditions described above and secondly with synchrotron X-ray at the Deutsches Elektronen-Synchrotron DESY.

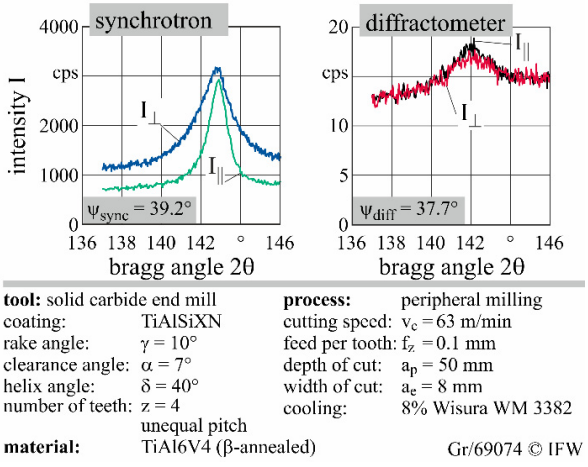

Fig. 2. diffractograms for synchrotron and diffractometer measurements

For this measurement the same wavelength as CuKα radiation was utilized: λ = 1.54 Å. An elliptic measurement focus of 16 x 4 mm² was set in comparison to the 2 mm diameter focus in the diffractometer. Figure 2 presents the diffractograms for the two methods parallel and orthogonal to the feed direction. The intensity for the synchrotron measurement is larger by a factor of 100 due to the larger beam cross section and the higher beam power. This enables a more precise peak identification for the lattice spacing determination and the subsequent stress calculation in comparison to the diffractometer measurement. The propagation of the lattice spacing values for the variation of $\sin^2\psi$ is to be seen in figure 3 for the synchrotron, standard diffractometry and three diffractometric measurements with enlarged measured sample area. According to the $\sin^2\psi$-method, the residual stress values are calculated from the slope of the strain over ψ. Therefore the regression coefficient R^2

$$R^2 = \frac{\sum_n \left(\varepsilon_{fit,lin} - \overline{\varepsilon_{meas}}\right)^2}{\sum_n \left(\varepsilon_{meas} - \overline{\varepsilon_{meas}}\right)^2} \quad (1)$$

for a linear approach is an important evaluation criterion for the comparison [9, 10].

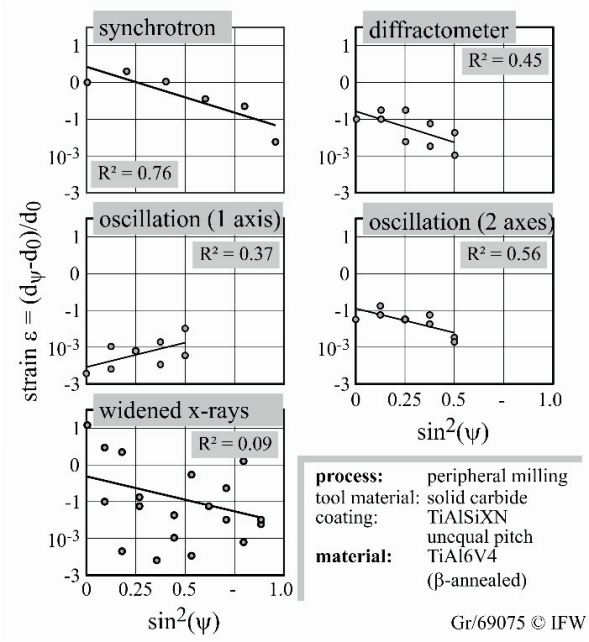

Fig. 3. comparison of measured lattice strain values

The standard diffractometric test reaches a correlation of $R^2 = 0.45$. This value can be improved to 0.56 via sample oscillation in 2 axes and 0.76 for the case of synchrotron measurement. However, the linear approximation for all cases is not sufficient. Therefore, methods based on changes in shape due to removal of parts of the sample, so called indirect methods, are analyzed in the following.

2.2. Indirect measurement methods

Indirect methods for residual stress determination base on measurement of shape changes due to removal of stress inherent material. Hole-drilling techniques as well as sectioning techniques are adoptable for planar samples, which are element of the present study. Hole-drilling methods provide reliable stress values from an information depth of t > 50 µm (for hole diameter d = 0.8 mm) and are therefore not applicable to determine process induced residual stresses typically having a high slope in this depth region. Therefore, the next chapter discusses sectioning techniques (layer removal methods) for the case of the investigated material Ti6Al4V in β-annealed state.

3. Layer removal method for residual stress determination

First discussions of residual stress determination based on the removal of stress inherent material were carried out by Cilley who investigated the deformation of removed material portions [11, 12]. However, these results are inaccurate due to the remaining stresses in the body material [6]. Therefore, Stäblein developed his equations for the removal of small material portions and for measuring at the remaining workpiece for the case of uniaxial stresses. Treuting and Read enhanced this for sheet materials with stresses constant in plane and varying in depth applicable for process induced residual stresses [13]:

$$\sigma_x(z_i) = \frac{-E}{6\cdot(1-\nu^2)} \cdot \left(\begin{array}{l} (z_0+z_i)^2 \left[\frac{d\varphi_x(z_i)}{dz_i} + \nu \cdot \frac{d\varphi_y(z_i)}{dz_i} \right] + \\ 4(z_0+z_i)\left[\varphi_x(z_i) + \nu\cdot\varphi_y(z_i)\right] - \\ 2\int_{z_i}^{z_0} \left[\varphi_x(z) + \nu\cdot\varphi_y(z) dz\right] \end{array} \right)$$

So far, applications of indirect stress determination utilize either electrochemical etching or cutting processes for the material removal. However, cutting processes require a minimum cutting depth to enable proper chip formation. This results in a depth resolution which is much larger compared to finishing processes such as electrochemical removal or laser machining which will be investigated in the following.

3.1. Electrochemical material removal

Electrochemical machining of titanium alloys is a common technology in the manufacturing of turbine parts. Here, pulsed electric current with high amperage is applied in saline electrolytes [14]. As a device capable of such functions was not available, process trials were carried out with decent current and voltage U = 9 V, and amperage I = 24 A using a circulation pump for electrolyte flow. According to VDI 3401 this process belongs to electrochemical polishing processes, which can be carried out with relatively simple devices [15]. As electrolyte, mixed saline solutions with sodium bromide and sodium nitrate (c_{NaBr} = 3.15 mol/l and c_{NaNO_3} = 1.26 mol/l) were used. Due to passivation, acidic solutions could not be used. An optimum concerning transport of the products of reaction, gas bubbles and attainable current density was determined at an electrode gap size of a = 5 mm (compare figure 5). Higher current densities enable better surface quality and equality of material removal while smaller gap sizes result in crater formation on the sample due to gas bubble formation covering the surface.

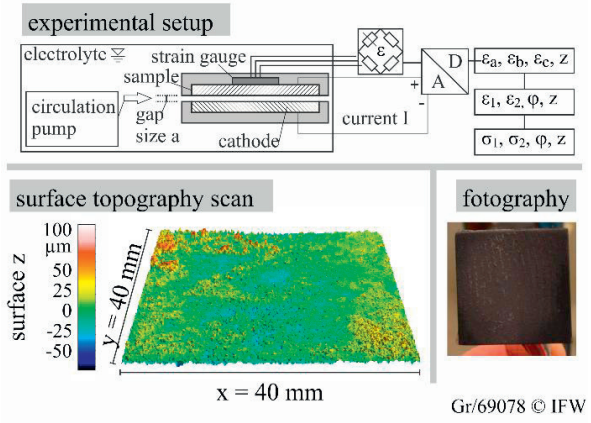

Fig. 4. surface topography of an electrochemically machined sample

As it can be seen from figure 4, the surface quality of the electrochemically machined samples is low. Due to gas bubble formation and the large material grain size the surface roughness according to ISO4287 is Rz = 19 µm (threshold wavelength λ_c = 0.8 mm). However, the material removal offers a linear behavior with respect to the amount of electricity, as displayed in figure 5. The regression function is utilized to calculate the measuring depth from the amount of electricity measured.

The sample preparation includes the application of the strain gauge as well as the electric bonding which has to be carried out on a large contact area to enable uniform electric flow in the material with lox conductivity. The contacting has to be isolated from the strain gauge as well as from the electrolyte resulting in an elaborate preparation effort.

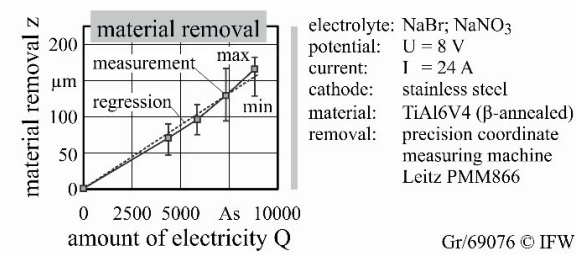

Fig. 5. experimental setup for electrochemical material removal and its removal behavior

3.2. Laser material removal method

For these reasons, laser material removal is investigated as an alternative method to ECM. In alteration of Treuting and Read's method, the strain on the backside of the sample is measured instead of the curvature φ using three-component strain gauges. This procedure enables the determination of main stresses and their direction. Most publications postulate the necessity for material removal processes avoiding the induction of new residual stresses. Some theoretical thoughts show, that laser ablation is an acceptable process under this aspect. The removal of stress inherent material layers results in a bending moment on a body:

$$M_{b,x} = \sum_i \underbrace{\left(\overline{\sigma_{x,i}} \cdot \Delta z_i \cdot b\right)}_{F_i} \cdot z_i$$

The resulting strain computes to:

$$\varepsilon_x = \frac{M_{b,x} - \nu \cdot M_{b,y}}{E \cdot I} \cdot z_i$$

If we now assume the induction of stresses by the laser material removal process, equation (3) is enhanced by a term for each layer removed:

$$M_{b,x,laser} = \left(\overline{\sigma_{x,laser}} \cdot \Delta z_{laser} \cdot b\right) \cdot z_i$$

Figure 6 presents the depth propagation of residual stresses measured with X-ray diffraction after laser material removal of a 7 x 7 mm² area on a 10 mm Ti6Al4V sample with fine grained bi-modal microstructure. Laser machining was carried out on a Sauer Lasertec 40 Precision machine tool. This machine is equipped with a Q-switch Nd:YVO_4 laser with a wavelength of λ = 1,064 nm (infrared). The process parameters feed velocity v_l, frequency f_l and laser power P_l were chosen on basis of a preliminary DOE-test (central-composite design) with the target values

productivity and removal depth: $v_l = 250$ mm/s, frequency $f_l = 25$ kHz and laser power $P_l = 6.5$ W. The trace offset was set to $o_t = 10$ µm and the process is carried out applying a unidirectional laser machining strategy resulting in a layer thickness of $\Delta z = 2.26$ µm. Tensile stresses are measured up to a depth of $z = 14$ µm.

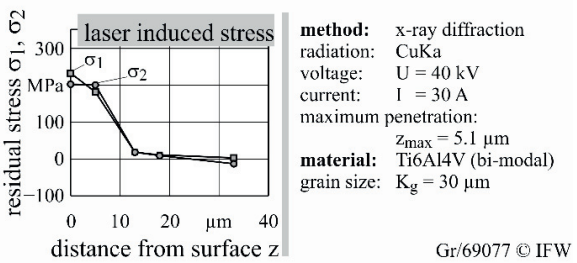

Fig. 6. residual stress depth profile after laser material removal

As it is unknown and cannot be measured (as discussed above) if these values are applicable to Ti6Al4V in β-annealed stage as well, a variation based on the measured values is carried out. For a constant mean stress value ($\sigma_{laser} = 144$ MPa) the penetration depth is varied by a factor of 0; 1; 10; 25; 100 and 200 compared to the measurement, figure 7 a). The stress value is varied by 0; 1; 2; 5; 7.5 and 10 for a constant depth of $z_{laser} = 14$ µm, figure 7 b).

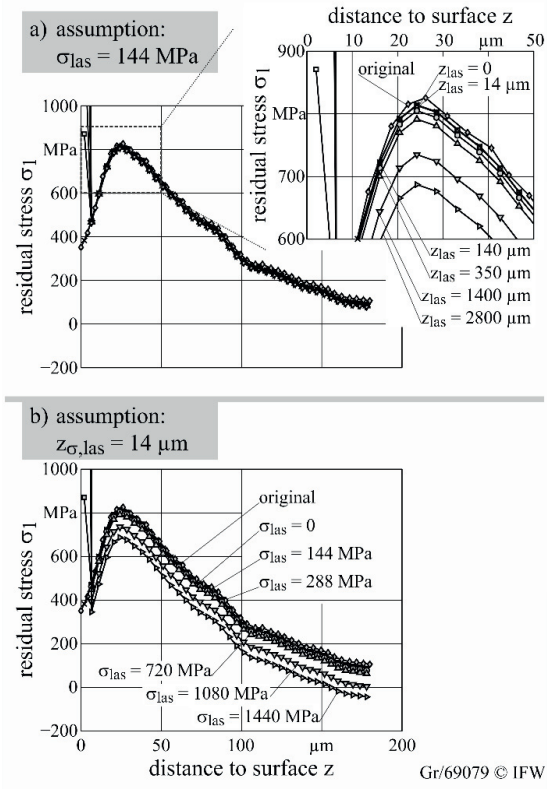

Fig. 7. residual stress depth profile after laser material removal

Afterwards the theoretical strain after layer wise material removal is calculated using equations (3)-(5) and the residual stresses are calculated using the equation from Treuting and Read (equation (2)). The resulting stress propagations are presented in figure 7. The maximum deviations between original and laser-superimposed residual stress propagation occur for the surface-near value and amount to $\Delta\sigma = \sigma_{laser,z1} - \sigma_{z1} = 50 \ldots 4677$ MPa for $\sigma_{laser} = 14 \ldots 1420$ MPa ($z_{laser} = 14$ µm) and to $\Delta\sigma = 242 \ldots 4819$ MPa for $z_{laser} = 7 \ldots 140$ µm ($\sigma_{laser} = 142$ MPa), respectively. These values are unacceptably high and widely exceed the material's strength. However, the deviation is minimal for the second value and increases only slightly with further depth ($\Delta\sigma_{z2\text{-}zn} < 20$ MPa). This value is comparable to the measurement accuracy of diffractometric determinations and therefore highly acceptable.

The removal behavior of laser ablation is linear. The layer thickness amounts to $\Delta z = 2.3$ µm enabling a good depth resolution of the stress measurement. Due to the linear movement of the laser front an unsteady temperature distribution results. Although the strain gauges utilized are temperature drift compensated for titanium, measurement deviation result due to this uneven distribution, compare strain propagations in figure 7. Room temperature at the sample bottom is reached after $t = 30$ s. However, constant strain values are measured only after $t = 260$ s. Therefore, a waiting time of $t_{wait} = 300$ s is utilized during laser removal experiments.

4. Approval of the indirect measuring methods

As a proof on concept, residual stresses after two milling experiments are measured using the two methods. Ti6Al4V is face milled using a Walter F4033 face mill with diameter $d = 130$ mm and $z = 16$ cutting inserts. The cutting velocity was $v_c = 30$ m/min, the feed per tooth $f_z = 0.15$ mm and the cutting depth $a_p = 1$ mm. The cutting inserts for the experiment analyzed with the electrochemical removal method were sharp and the experiment was carried out once. Cutting edges for cutting experiment for the laser ablation method were worn (average flank wear land VB = 80 µm) and five samples were milled to analyze repeatability. Figure 8 shows the results of these experiments by means of the two main stresses.

The residual stress values for the laser ablation method show large tensile stresses in surface near material. Their absolute values vary by $\Delta\sigma_{1,surface} = 120$ MPa and $\Delta\sigma_{2,surface} = 690$ MPa. Maximum values are to be found in the pressure domain. Absolute values differ between $\sigma_1 = 520\text{-}820$ MPa and $\sigma_2 = 525\text{-}705$ MPa and are located in a depth of

$z_{\sigma,max}$ = 10-20 µm. The maximum penetration depth is found to be z_{max} = 30 µm. Although a wide range of maximum values is determined, the repeatability can be rated as very good, as all five propagations show identic tendencies and zero-crossings. For the objective of distortion prediction, the quality of the analysis results is sufficient. The stress propagations for electrochemical measurement differ from the laser ones due to the tool wear state. Only compressive stresses are measured due to a reduced thermal load in the cutting process caused by sharp cutting edges.

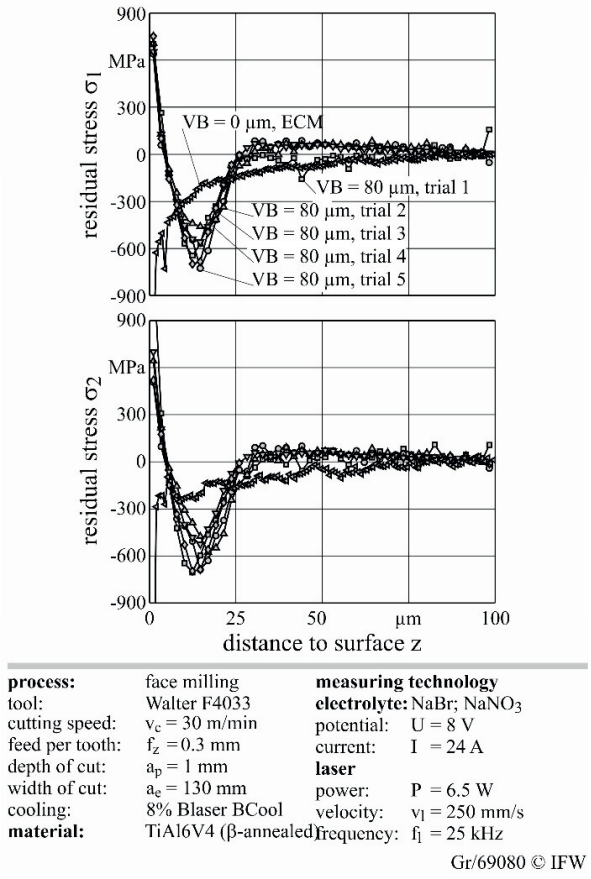

Fig. 8. residual stress depth profile after laser material removal

5. Summary

For some applications, such as large grained metals, direct measurement methods for the determination of residual stresses are not applicable. For this reason, indirect measurement methods have been presented on this paper based on the method of Treuting & Read. Laser material removal and electrochemical etching have been discussed as material removal processes. Laser material removal offers precise results and possesses advantages with respect to sample preparation and data analysis. Although maximum data variation is very high, the method can be used for stress analysis with respect to distortion prediction as principal stress propagation can be measured with decent precision.

Acknowledgements

The presented investigations were undertaken with support of the Lower Saxony Ministry for Economics, Labour and Transport within the project: “Verfahren zur Modellierung der Einflüsse auf die Werkstückgestalt bei der Fräsbearbeitung von Titan” (QualiTi WB3-80121829). The authors thank Premium Aerotec GmbH, Varel, Germany for the cooperation within this project and the Deutsches Elektronen-Synchrotron DESY in Hamburg for the synchrotron residual stress measurements.

References

[1] McQuillan, A. D., McQuillan, M. K., 1956. Titanium, no. 4 in Metallurgy of the rarer metals, Butterworths, London.
[2] Dege, J. H., 2012. High performance machining of large titanium structural parts, in: New macnufacturing technologies in aerospace industry, Hannover.
[3] Leyens, C., Peters, M., 2003, Titanium and titanium alloys, Wiley.
[4] Donachie, M. J., 2000. Titanium, 2nd Edition, ASM International, Materials Park, Ohio.
[5] Lütjering, G., Williams, J. C., 2007. Titanium, 2nd Edition, Engineering materials and processes, Springer, Berlin.
[6] Brinksmeier, E., Cammett, J., König, W., Leskovar, P., Peters, J., Tönshoff, H. K., 1982. Residual stresses — measurement and causes in machining processes, CIRP Annals 31 (2), pp 491 – 510.
[7] Rossini, N., Dassisti, M., Benyounis, K., Olabi, A., 2012. Methods of measuring residual stresses in components, Materials & Design 35 (0), pp. 572 – 588.
[8] Tönshoff, H. K. 1966. Eigenspannungen und plastische Verformungen im Werkstück durch spanende Bearbeitung [Residual stresses and plastic work piece deformation due to machining], Dr.-Ing. Diss., Hannover.
[9] Breidenstein, B., 2011. Oberflächen und Randzonen hoch belasteter Bauteile [Surfaces and subsurfaces of highly strengthened components], Postdoctoral lecture qualification, Leibniz Univeristät Hannover.
[10] Macherauch, P., Müller, E., 1961. Das $\sin^2\psi$-Verfahren der röntgenographischen Spannungsmessung [The $\sin^2\psi$-method for X-ray stress measurement], Zeitschrift für angewandte Physik, pp. 305–312.
[11] Stäblein, F., 1931. Spannungsmessungen an einseitig abgelöschten Knüppeln [Stress measurement of one side quenched billets], Krupp’sche Monatshefte 12, pp. 93–99.
[12] Cilley, F., 1901. Some fundamental propositions in the theory of elasticity. A study of primary or self-balancing stresses, American Journal of Science 11, pp. 269–290.
[13] Treuting, R. G., Read, W. T., 1951. A mechanical determination of biaxial residual stress in sheet materials, Journal of Applied Physics 22 (2), pp. 130–134.
[14] Rajurkar, K., Sundaram, M., Malshe, A., 2013. Review of electrochemical and electrodischarge machining, in Proceedings of the 17th CIRP Conference on Electro Physical and Chemical Machining, pp. 13 – 26.

[15] VDI 3401, 2009. Elektrochemisches Abtragen – Formabtragen [Electrochemical machinig – EC-forming].